

# Pulse Skipping Modulation Method for Multiple Input Buck Boost Converter

Son Nguyen<sup>1</sup>, Kelvin Yuk<sup>2</sup>, Rajeevan Amirtharajah<sup>1</sup>

<sup>1</sup>Department of Electrical and Computer Engineering, University of California, Davis, CA, USA

<sup>2</sup>Echoic Engineering LLC, San Francisco, CA 94134

sohnguyen@ucdavis.edu

**Abstract**—Energy harvesting and wireless power transfer to power small, low-power and autonomous devices have recently attracted numerous research studies. Due to the lack of energy supplies, DC to DC converters with multiple inputs have been studied to harvest different energy sources simultaneously. In this paper, a proposed pulse skipping modulation method is used to control a multiple input buck boost converter with the output power from 7  $\mu\text{W}$  – 700  $\mu\text{W}$ . The DC to DC converter can achieve a high efficiency of 83.3% at 23.6  $\mu\text{A}$  load current, and the highest efficiency is up to 89.1% at 255  $\mu\text{A}$  current load. The control method offers the flexibility and adaptability in maximum power point tracking and input power contribution. The paper investigates a completed energy harvesting system including a solar cell and 915 MHz RF source and power management circuits.

**Keywords**—Pulse Skipping Modulation, Buck converter, Boost Converter, Energy Harvesting, DC to DC converter.

## I. INTRODUCTION

Recent developments in wireless applications and RF devices have significantly changed the world. The new trend of RF energy harvesting and wireless power transfer enables RF systems to not only receive and process the RF signals but also turn those RF signals into energy. That the IoT sensors consume low power due to the long time duration between wireless charging cycles allows RF energy harvesting and wireless power transfer to fully power sensors and wearable devices and remotely recharge device batteries. The greatest challenge of energy harvesting and wireless power transfer is sufficiently harnessing ambient energy sources to power low-power electronic circuits or sensors. Different papers focused on improving the transducer performance by using large-dimension transducers [1] and [2], reducing the distance from the transducers with wireless inductance coils to RF sources in [3]–[5] or designing hybrid structures which can scavenge multiple energies simultaneously [6]–[9]. Other works [10]–[12] mainly researched on increasing the efficiency of power management circuits which include AC to DC and DC to DC converters.

Energy harvesting systems harvest very small power on the order of microwatts to milliwatts. As a result, the buck and boost converters normally operate in a discontinuous conduction mode in which the duty cycle of switching in inductive-based converters is small (from 1% to 20%). The converter inductor is charged or discharged in small intervals

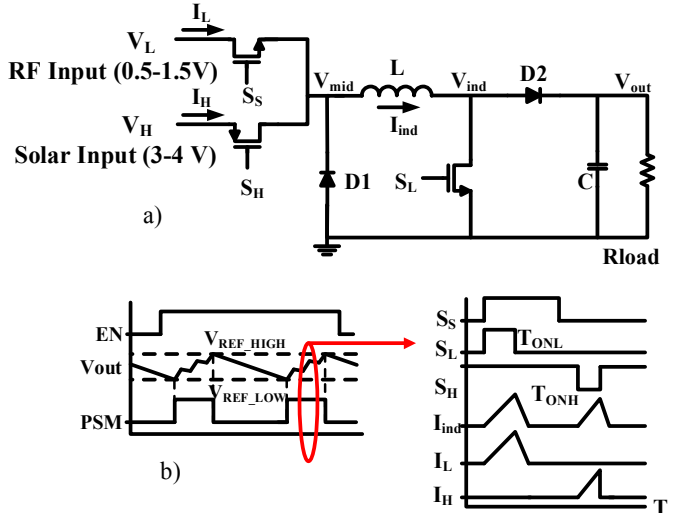


Fig. 1. a) Multiple input buck boost converter and b) pulse skipping modulation timing diagram.

and is not used during the rest of the switching period. Consequently, the inductor can be used for other purposes to deliver power from other energy sources. From this idea, this paper presents a pulse skipping modulation (PSM) method to control a multiple input buck boost configuration to simultaneously harvest energy from both solar and radio frequency (RF) sources. Several papers [13] and [14] presented pulse width modulation methods to control multiple input converters; however, tracking maximum power points and equally distributing the harvested power among the inputs require high power and more complex control circuits. This paper uses a simplified algorithm of the PSM method which allows a low-power control circuit designed for energy harvesting system.

Section I of this paper has introduced the overview of energy harvesting and the proposed the control approach. The pulse skipping modulation method for a multiple input buck boost converter is discussed in Section II. Section III shows experimental results of the tested converter system. Finally, some conclusions summarize the achievements of this paper and future work.

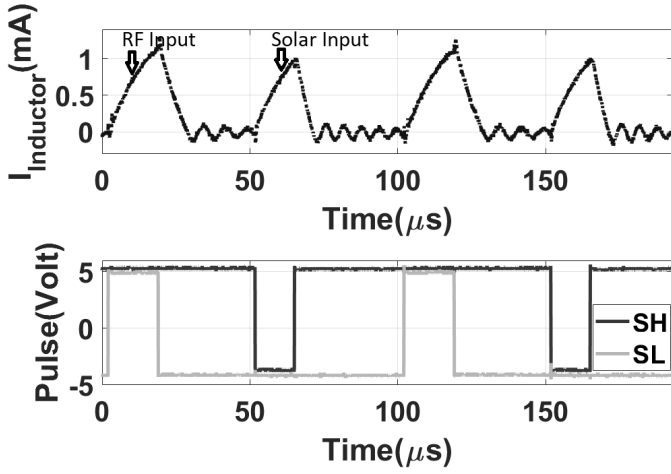


Fig. 2. Inductor current with switching pulses.

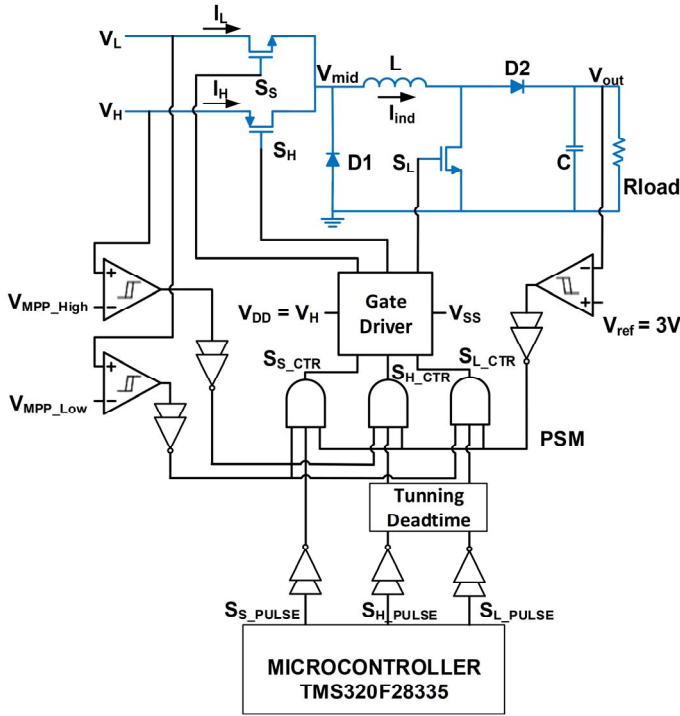


Fig. 3. The PSM controlling system of multiple input buck boost converter.

## II. PSM FOR MULTIPLE INPUT BUCK BOOST CONVERTER

The configuration of the multiple input buck boost converter is illustrated in Fig. 1a). The converter has two inputs: low-voltage (from the RF to DC converter output) and high-voltage (from a solar cell output). The converter is a combination of buck and boost converters. All MOSFET switches in the converter are controlled by switching signals  $S_L$ ,  $S_H$  and  $S_S$ . The signals contained within the pulse skipping modulation phase are shown in Fig. 1b). The output voltage is compared to a reference voltage using a hysteresis comparator. When  $V_{\text{out}}$  is smaller than  $V_{\text{REF\_LOW}}$ , the PSM signal goes high to generate the switching pulses for all of the MOSFET switches  $S_L$ ,

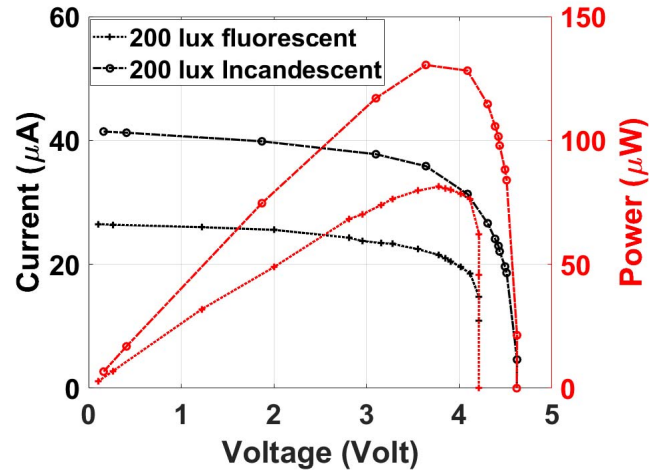


Fig. 4. Output Current and power versus voltage of a solar cell.

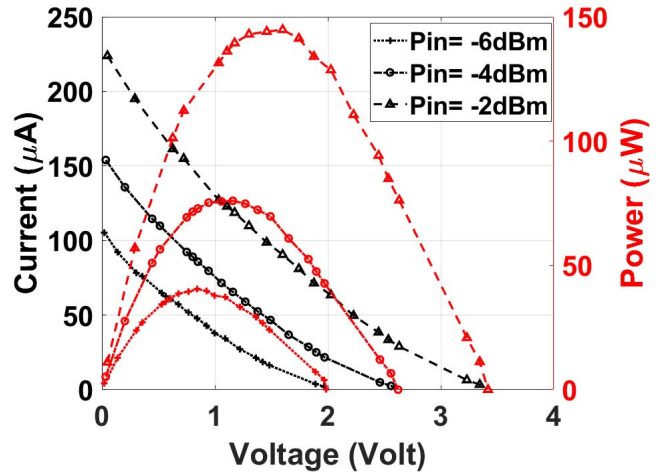


Fig. 5. Output Current and power versus voltage of RF to DC converter.

$S_H$  and  $S_S$ , until  $V_{\text{out}}$  reaches  $V_{\text{REF\_HIGH}}$ . The switching signals are turned off when  $V_{\text{out}}$  reduces from  $V_{\text{REF\_HIGH}}$  to  $V_{\text{REF\_LOW}}$ . The PSM method offers high efficiency due to reducing switching and conduction loss but causes large output voltage ripple. Fig. 1b) and 2 shows the sequential switching signals. There are two intervals for boost and buck conversions in one switching period in which the  $S_S$  switch is used to prevent a current flowing from the  $V_H$  input to the  $V_L$  input when  $S_H$  is ON. In the first half of the switching period (when  $S_S$  is ON),  $S_L$  is utilized in boost conversion to deliver power from the low-voltage  $V_L$  input into the load through an inductor  $L$ . When  $S_L$  turns on, the inductor current  $I_{\text{ind}}$  increases, and when  $S_L$  turns off, diode  $D2$  is ON so that all the charge from the inductor is transferred into the load. Similarly, the second half of the switching period is used for the buck conversion process.  $S_H$  is controlled by a switching pulse to deliver the power from the high-voltage  $V_H$  input into the output load. In the PSM approach, the switching period and duty cycles are controlled such that the converter operates in discontinuous conduction mode. Figure 2 shows the measurements of the inductor current corresponding to the pulse switching signals.

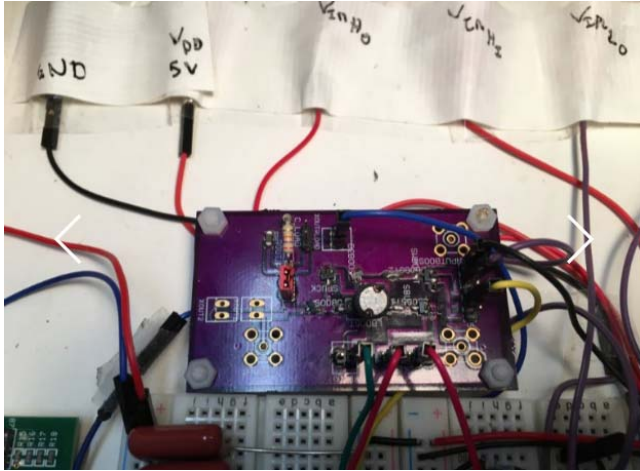


Fig. 6. The fabricated multiple input buck boost converter.

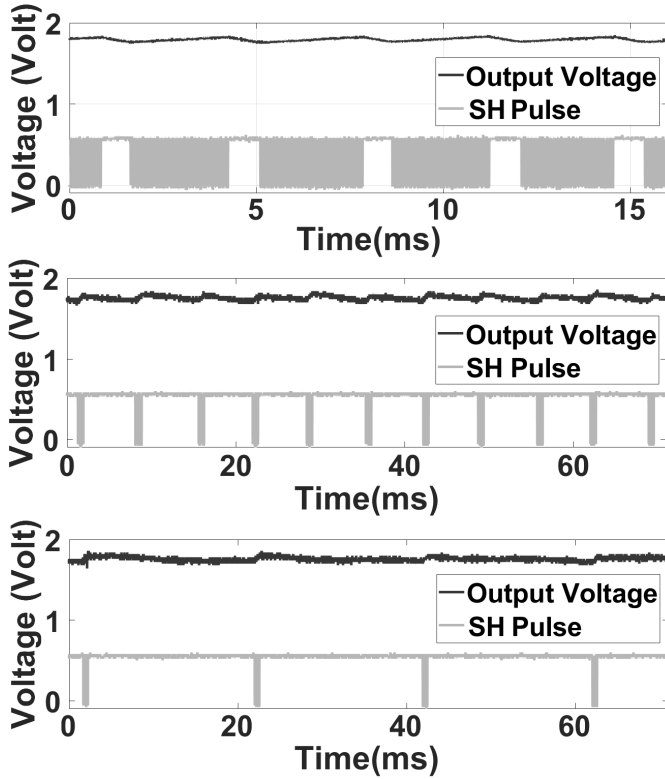


Fig. 7. Output voltage and SH switching pulse of the DC to DC converter with 6.8 kOhm (top), 56 kOhm (middle) and 220 kOhm (bottom) load.

Figure 3 illustrates the detailed PSM control system. A microcontroller is used to generate the switching outputs with adjustable duty cycles which are connected to different delay blocks to prevent the switching pulse from overlapping. The circuit also provides the maximum power point tracking by comparing the converter inputs with two reference voltages using two comparators. To fully turn on and off all MOSFET switches, the level shifter and gate driver are used to generate output pulses switching from  $V_{SS}$  to  $V_H$ . For instance, when D1 is ON in Fig. 3, the voltage at the  $V_{mid}$  node goes lower than zero; therefore, a negative voltage  $V_{SS}$  is applied to the  $S_H$  gate to turn off the  $S_S$  switch.

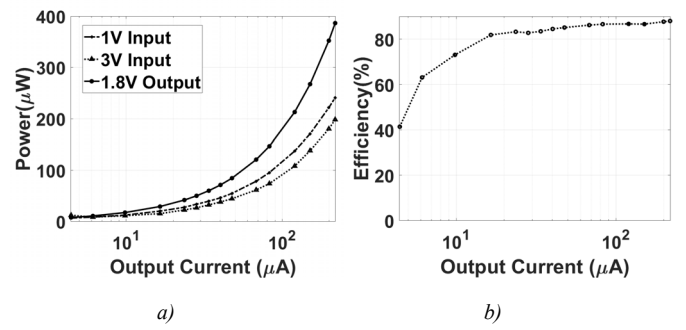


Fig. 8 a) Input and output powers versus output current b) the efficiency of the converter with different output current.

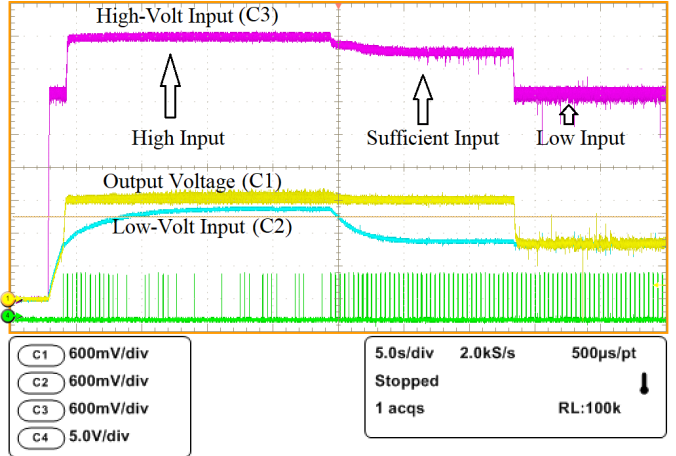


Fig. 9. The output voltage behavior with different input conditions.

### III. EXPERIMENTAL RESULTS

The multiple input buck boost converter system including an RF generator, RF to DC converter, a solar source, and DC to DC converter is implemented and tested. The outputs of a solar cell and an RF to DC converter are connected to the high and low voltage inputs of the converter, respectively. The switching pulses of the converter MOSFETs are generated and controlled by Texas Instruments MCUs TMS320F28335 and discrete control circuits. This section discusses the experimental results of the energy harvesting interface circuits.

#### A. Solar and RF to DC Outputs

The Panasonic AM-1801 25 x 53 mm solar cell was used to generate a high voltage input with a maximum power point (MPP) of approximately 3.7 V. The solar cell is tested under incandescent and fluorescent lamps which simulate outdoor and indoor lighting, respectively. With the same 200 lux illumination, the solar cell using incandescent light can generate 49  $\mu$ W higher than that using fluorescent light as shown in Fig. 4. The  $V_L$  input of the converter is supplied by a 915 MHz RF to DC system consisting of an RF signal generator, a matching network [15] and a 6-stage Cockcroft-Walton RF to DC converter [16]. When the RF input power increases from -6 dBm to -2 dBm, the maximum output DC power produced ranges from 40  $\mu$ W to 145  $\mu$ W. Figure 5 demonstrates that the MPP of the output of RF to DC

converters approximately equals to 46.8% of the open-circuit voltage.

### B. System Measurements

The fabricated multiple input buck boost circuit is shown in Fig. 6. The chosen low voltage drop and power loss Schottky diode, PMOS and NMOS switches are BAT754, BSS138, and NTR1P02L, respectively. The fixed switching pulse duties of MOSFET  $S_L$  and  $S_H$  are 17% and 13% of the switching period of 1  $\mu$ s. The inductor value is 10 mH, and the output capacitor is 10  $\mu$ F. The pulse density and output voltage ripple in PSM control depend on the output load conditions. Figure 7 shows the transient behavior of  $V_{out}$  under various load conditions:  $R_{Load}=6.8$  kOhm, 56 kOhm and 220 kOhm. When the load resistance increases, the switching pulse density and  $V_{out}$  ripple increase. For  $R_{Load}=8$  kOhm and using an average output voltage of 1.8V and constant supply voltages of 1V and 3V, the output ripple is 65 mVpp. The distributed power consumption of two inputs and the output power and efficiency are illustrated in Fig. 8. The maximum efficiency of the multiple input converter reaches up to 89%. The converter maintains a high efficiency of 63% at a low output current of 6  $\mu$ A. The calculated efficiency does not take into account the power required for the control circuits and microcontroller which can be minimized when using optimized integrated circuits. The converter can operate with output power in the range of 7  $\mu$ W – 700  $\mu$ W.

Finally, Fig. 9 illustrates the adaptability of the converter controlled by the PSM approach when input conditions are changed. When the total input power from light and RF is abundant and much larger than the needed input, the output voltages of solar cell and RF to DC converter go toward the open-circuit voltages ( $V_H= 4.1$  V and  $V_L=1.4$  V). When an input power decreases but is still sufficient, the supply voltages reach close to the controlled MPPs. If the total input is not enough to power the load, the inputs are maintained at the MPPs while the output voltage is reduced.

## IV. CONCLUSIONS

This paper has shown a proposed pulse skipping modulation method to control a complete multiple input buck boost converter for RF and solar energy harvesting. The converter can work in the output power range of 7  $\mu$ W to 700  $\mu$ W with the maximum efficiency up to 89%. This work also presents a MPP tracking which can adapt to different load and input conditions. Future work will complete the converter by designing an IC tape-out of the controlling circuits to increase the system efficiency and reduce power loss.

## ACKNOWLEDGMENT

S. Nguyen was supported by Vietnam Education Foundation fellowship and a Google Faculty Research Award. The authors would like to thank R. Bhardwaj at Google-X for his feedback and supports.

## REFERENCES

- [1] C. C. Kang, S. S. Olokede, N. M. Mahyuddin and M. F. Ain, "Radio frequency energy harvesting using circular spiral inductor antenna," WAMICON 2014, Tampa, FL, 2014, pp. 1-5.
- [2] M. J. M. Silva, M. S. R. Palacios, A. M. R. Diaz and L. B. M. Rincón, "Radio frequency energy harvesting using series resonant circuit," 2017 IEEE 18th Wireless and Microwave Technology Conference (WAMICON), Cocoa Beach, FL, 2017, pp. 1-4.
- [3] Y. Zou and S. O'Driscoll, "Implant Position Estimation Via Wireless Power Link," in IEEE Transactions on Circuits and Systems II: Express Briefs, vol. 62, no. 2, pp. 139-143, Feb. 2015.
- [4] C. Van Pham, A. V. Pham and C. S. Gardner, "Development of Helical circular coils for wireless through-metal inductive power transfer," 2017 IEEE Wireless Power Transfer Conference (WPTC), Taipei, 2017, pp. 1-3.
- [5] M. Tian, N. Wang, K. Wang, H. Jia, Z. Li, X. Yang and L. Wang "A wire-embedded converter used for wearable devices," 2017 IEEE Applied Power Electronics Conference and Exposition (APEC), Tampa, FL, 2017, pp. 121-125.
- [6] S. H. Nguyen, R. Amirtharajah, "A Hybrid RF and Vibration Energy Harvester for Wearable Devices," in 2018 IEEE Applied Power Electronics Conference and Exposition, March, 2018, in press.
- [7] S. H. Nguyen, Kelvin Yuk, R. Amirtharajah, and George R. Branner, "Radiation Patterns of an RF Energy Harvesting Necklace on Human Body Phantom," 2018 IEEE International Symposium on Antennas and Propagation, Boston, MA, July 2018, in press.
- [8] A. Collado and A. Georgiadis, "Conformal Hybrid Solar and Electromagnetic (EM) Energy Harvesting Rectenna," in IEEE Transactions on Circuits and Systems I: Regular Papers, vol. 60, no. 8, pp. 2225-2234, Aug. 2013.
- [9] S. Lemey, F. Declercq and H. Rogier, "Textile Antennas as Hybrid Energy-Harvesting Platforms," in Proceedings of the IEEE, vol. 102, no. 11, pp. 1833-1857, Nov. 2014.
- [10] E. Lefevre, D. Audigier, C. Richard and D. Guyomar, "Buck-Boost Converter for Sensorless Power Optimization of Piezoelectric Energy Harvester," in IEEE Transactions on Power Electronics, vol. 22, no. 5, pp. 2018-2025, Sept. 2007.
- [11] M. M. Ababneh, S. Perez and S. Thomas, "Optimized power management circuit for RF energy harvesting system," 2017 IEEE 18th Wireless and Microwave Technology Conference (WAMICON), Cocoa Beach, FL, 2017, pp. 1-4.
- [12] D. El-Damak and A. P. Chandrakasan, "A 10 nW–1  $\mu$ W Power Management IC With Integrated Battery Management and Self-Startup for Energy Harvesting Applications," in IEEE Journal of Solid-State Circuits, vol. 51, no. 4, pp. 943-954, April 2016.
- [13] C. Shi, B. Miller, K. Mayaram and T. Fiez, "A Multiple-Input Boost Converter for Low-Power Energy Harvesting," in IEEE Transactions on Circuits and Systems II: Express Briefs, vol. 58, no. 12, pp. 827-831, Dec. 2011.
- [14] Z. Li, O. Onar, A. Khaligh and E. Schaltz, "Design and Control of a Multiple Input DC/DC Converter for Battery/Ultra-capacitor Based Electric Vehicle Power System," 2009 Twenty-Fourth Annual IEEE Applied Power Electronics Conference and Exposition, Washington, DC, 2009, pp. 591-596.
- [15] D. P. Nguyen, J. Curtis and A. V. Pham, "A Doherty Amplifier With Modified Load Modulation Scheme Based on Load-Pull Data," in IEEE Transactions on Microwave Theory and Techniques, vol. 66, no. 1, pp. 227-236, Jan. 2018.
- [16] S. H. Nguyen, N. Ellis and R. Amirtharajah, "Powering smart jewelry using an RF energy harvesting necklace," 2016 IEEE MTT-S International Microwave Symposium (IMS), San Francisco, CA, 2016, pp. 1-4.